

SPECTRAL SHAPE VARIATION OF INTERSTELLAR ELECTRONS  
AT HIGH ENERGIES

L.C.Tan  
Department of Physics and Astronomy  
University of Maryland  
College Park, MD 20742  
USA

Our analysis of the high-energy electron spectrum has shown that the electron intensity inside the  $H_2$  cloud region, or in a spiral arm, should be much lower than that outside it and the observed electron energy spectrum should flatten again at about 1 TeV.

In the framework of the leaky box model the recently established rigidity ( $R$ ) dependence of the escape pathlength ( $\lambda_e$ ) of cosmic rays (i.e.,  $\lambda_e \propto R^{-0.7}$ ) (1) would predict a high-energy electron spectrum which is flatter than the observed one. We explain this divergence by assuming that the leaky box model can only apply to cosmic-ray heavy nuclei, and light nuclei and electrons in cosmic rays may have different behaviours in the interstellar propagation. Therefore, the measured data on high-energy electrons should be analyzed based on our proposed nonuniform galactic disk (NUGD) model (2).

In the NUGD model (see Fig. 1 of OG 7.2-10) Box 1 and Box 2 are the confinement volumes of primary nuclei and electrons in the solar vicinity and above the  $H_2$  cloud region respectively, Box II is the dense  $H_2$  cloud region and Box I represents the magnetic tube located in the central layer of the Orion arm. The  $H_2$  cloud region is assumed to be inert, hence primary nuclei and electrons should originate from Box 1 (the local component) or Box 2 (the distant component). Hereafter we use the subscripts 1, 2, I and II to express the quantities referred to Boxes 1, 2, I and II respectively.

By using Gauss's theorem, we have

$$\frac{1}{V_2} \int_{s_2} \vec{J}_{i2} \cdot \vec{n}_2 ds_2 = \frac{1}{V_2} \int_{V_2} \nabla \cdot \vec{J}_{i2} dr_2^3, \quad (1)$$

where  $\vec{J}_{i2}$  is the net flow of the  $i$ th kind of particles in the coordinate space ( $r_2$ ) of Box 2,  $V$ ,  $s$  and  $\vec{n}$  are the volume, the surface area and the unit vector normal to  $s$  respectively. According to the 'leaky box' concept the right hand side of Eq. (1) may be replaced by  $N_{i2}/\tau_{e2}$ , where  $\tau_{e2}$  is the mean escape lifetime of cosmic rays. Since

$$s_2 = s_{2 \rightarrow II} + s_{2 \rightarrow \text{halo}}, \quad (2)$$

where  $s_{2 \rightarrow II}$  and  $s_{2 \rightarrow \text{halo}}$  are the area of the boundaries between Box 2 and Box II and Box 2 and the halo respectively, we can write

$$\int_{s_{2 \rightarrow II}} \vec{J}_{i2} \cdot \vec{n}_2 ds_2 + \int_{s_{2 \rightarrow \text{halo}}} \vec{J}_{i2} \cdot \vec{n}_2 ds_2 = \frac{V_2 N_{i2}}{\tau_{e2}}, \quad (3)$$

We define the first and second terms on the left hand side of Eq. (3) as  $V_2 N_{i2} / \tau_{e2 \rightarrow II}$  and  $V_2 N_{i2} / \tau_{e2 \rightarrow \text{halo}}$  respectively.

Here the quantity

$$\frac{1}{V_{II}} \int_{s_{2 \rightarrow II}} \vec{J}_{i2} \cdot \vec{n}_2 ds_2$$

is just the source term of the  $i$ th kind of particles in Box II due to the flow from Box 2,  $q_{iIII}$ ,

$$q_{iIII} = \frac{1}{V_{II}} \int_{s_{2 \rightarrow II}} \vec{J}_{i2} \cdot \vec{n}_2 ds_2 = \frac{m \bar{n}_2 \beta c V_2}{V_{II}} \frac{N_{i2}}{\lambda_{e2 \rightarrow II}} \quad (4)$$

Here we have used

$$\lambda_e = m \bar{n} \beta c \tau_e, \quad (5)$$

where  $m$  is the proton mass,  $\beta c$  is the particle velocity and  $\bar{n}$  is the mean matter density of the ISM. As  $\lambda_{e2}$  is independent of the nature of the particles, from Eq. (3)  $\lambda_{e2 \rightarrow II}$  should also be independent of the nature of the particles. Therefore, in order to estimate  $q_{iIII}$  we only need to consider the main proton component of cosmic rays, which has the continuity equation in Box II at high energies,

$$N_{pII} \left( \frac{1}{\lambda_{eII}} + \frac{1}{\lambda_p^i} \right) = \frac{m \bar{n}_2 c V_2}{V_{II}} \frac{N_{p2}}{\lambda_{e2 \rightarrow II}} + \int_E^\infty \frac{1}{\lambda_p^i} \frac{dN_p(E', E')}{dE_p} N_{pII}(E') dE'_p, \quad (6)$$

where  $\lambda_p^i$  is the mean inelastic interaction length of interstellar protons and  $dN_p/dE = 1/E'$  is the energy distribution of protons after their inelastic interactions. Under the power-law approximation ( $N_p \propto E_p^{-\gamma_p}$ ) we can get

$$\lambda_{e2 \rightarrow II} = \frac{m \bar{n}_2 c V_2 \lambda_{pII}^{eff}}{V_{II}} \frac{N_{p2}}{N_{pII}}, \quad (7)$$

where  $\lambda_{pII}^{eff} = 1 / \left( \frac{1}{\lambda_{eII}} + \frac{1}{\lambda_p^{att}} \right)$  and  $\lambda_p^{att} = \lambda_p^i / (1 - 1/\gamma_p)$ . Owing to the

fact that no cosmic-ray gradient exists in the inner Galaxy, the condition  $N_{p2} = N_{pII}$  should be held. Then by combining Eqs. (4) and (8) we have

$$q_{iIII} = N_{i2} / \lambda_{pII}^{eff}. \quad (8)$$

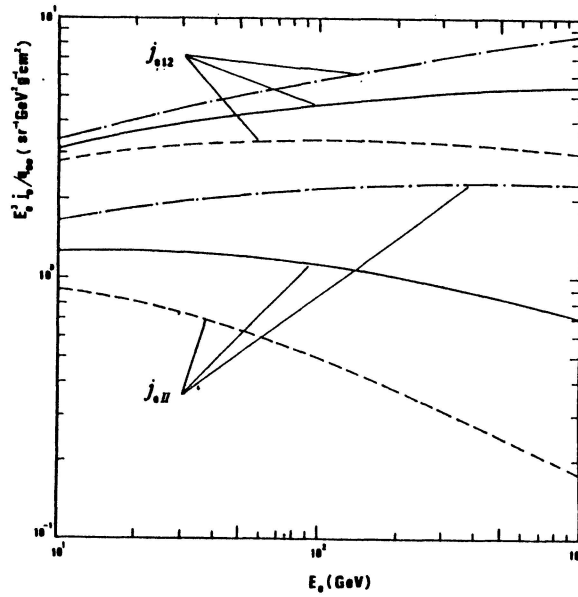


Fig. 1

Assuming that cosmic-ray electrons originate from a shock acceleration process, at high energies we should take their source term  $q_{e2}$  ( $=q_{e1} \propto E^{-2}$ ) and their intensity  $N_{e2}$  ( $=N_{e1} \propto E^{-3}$ ) due to electromagnetic losses. From Eqs. (7)-(8) we get

$$\lambda_{pII}^{eff} \propto \lambda_{eII} \propto E^{-0.7},$$

$$q_{eII} \propto E^{-2.3} \text{ and } N_{eII} \propto E^{-3.3},$$

which is fully consistent with recent observations. Thus our deduced  $j_{e12}$  and  $j_{eII}$  are shown in Fig. 1, in which the dot-dashed lines, the solid lines and the dashed lines represent the cases of  $\delta = 0.8, 0.7$  and  $0.6$  respectively. From Fig. 1 it is immediately noted that the electron flux in the  $H_2$  cloud region (and hence in the solar neighbourhood) should be much less than that in the distant regions (Boxes 1 and 2). Actually, this prediction is consistent with the observation(3).

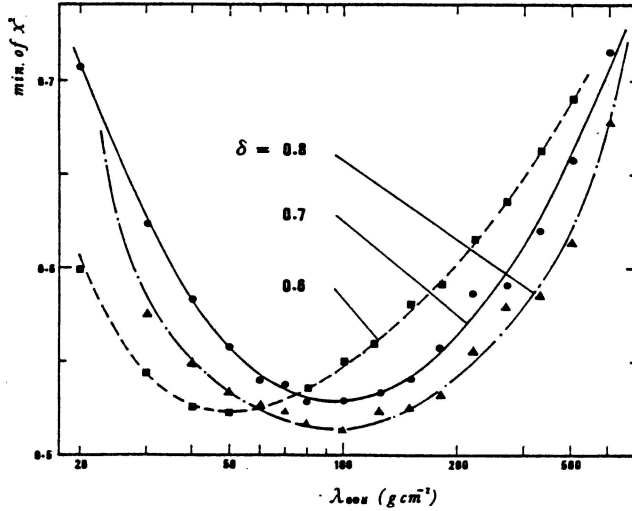


Fig. 2

Further, the attenuation factor of high-energy electrons along the magnetic tube (Box I) before reaching the solar neighbourhood is

$$\eta = \exp ((\gamma_{eII} - 2) \ln(1 - \alpha)), \tag{10}$$

where  $\gamma_e$  is the spectral index of the electron spectrum,  $\alpha = bE x_{Is}$ ,  $x_{Is}$  being the pathlength of electrons in Box I to reach the solar neighbourhood, and  $b = 7 \times 10^{-3} (\text{GeV}^{-1} \text{g}^{-1} \text{cm}^2)$ (4). Thus the predicted electron intensity in the solar neighbourhood should be

$$N_{ep} = (1 - \epsilon) \eta N_{eII} + \epsilon N_{e12}, \tag{11}$$

where  $\epsilon$  is the fraction of protons coming from Box 1 in the observed proton flux.

Recent data on high-energy electrons (5)-(7) have been used to estimate astrophysical parameters inherent in the NUGD model. In Fig. 2 we show a plot of the minimum  $\chi^2$  value, which is obtained by varying  $q_{e0}$  (the source term  $q_{e12} = q_{e0} E^{-\gamma_s}$  and  $\gamma_s + \delta = 2.75$ ) and  $\epsilon$  simultaneously, against  $\lambda_{e0II}$  ( $\lambda_{eII} = \lambda_{e0II} E^{-\delta}$ ). From this plot the allowable range of  $\lambda_{e0II}$  can be established.

In Table 1 we list the values of some model parameters estimated from our  $\chi^2$  fitting procedure. It is noticeable that  $\epsilon = 5 \pm 1 \%$ , indicating that the dominant part of observed cosmic-ray protons should come from the  $H_2$  cloud region. Moreover, the deduced  $\lambda_{e0II} / \lambda_{e012} \approx 3$  at  $\delta = 0.7$ , which is also consistent with our previous conclusion that most of secondary antiprotons should be produced in the  $H_2$  cloud region(2).

In the magnetic tube (Box I) the diffusion coefficient of 10 GeV cosmic rays is estimated to be about  $10^{30} \text{ cm}^2 \text{ s}^{-1}$ , which corresponds their mean free path of about 50 pc. This is consistent with the assumption that the scattering of cosmic rays by hydromagnetic waves should happen in the zone outside an arm, while along an arm there should be a free zone where cosmic rays are free to stream along the field lines with speeds of the order of the velocity of light(8).

Finally, in Fig.3 we show the electron fluxes predicted for the NUGD model (see the explanation of the curves shown in Fig.2). It is noticeable that the predicted electron spectra for all the  $\delta$  values considered exhibit a flattening at about 1 TeV. This flattening is understandable because at very high-energies observed electrons should only originate from their

$\delta$	$x_{0I}/\lambda_p^A$	$\epsilon$ (%)	$\frac{g_{e0}}{10^2 \text{ m}^{-2} \text{ s}^{-1} \text{ GeV}^{-1} \text{ g}^{-1} \text{ cm}^2}$	$\lambda_{e012}$ ( $10^6 \text{ gcm}^{-2}$ )	$\lambda_{e011}$ ( $10^6 \text{ gcm}^{-2}$ )
0.8	0.9	4	3.1 $\begin{smallmatrix} +1.9 \\ -1.1 \end{smallmatrix}$	3.5 $\begin{smallmatrix} +3.0 \\ -1.3 \end{smallmatrix}$	1.0 $\begin{smallmatrix} +1.2 \\ -0.6 \end{smallmatrix}$
0.7	0.4	5	3.1 $\begin{smallmatrix} +1.8 \\ -0.9 \end{smallmatrix}$	4.0 $\begin{smallmatrix} +4.0 \\ -1.7 \end{smallmatrix}$	1.0 $\begin{smallmatrix} +1.0 \\ -0.5 \end{smallmatrix}$
0.6	0.1	6	2.4 $\begin{smallmatrix} +1.4 \\ -0.5 \end{smallmatrix}$	5.6 $\begin{smallmatrix} +6.0 \\ -2.5 \end{smallmatrix}$	0.5 $\begin{smallmatrix} +0.7 \\ -0.2 \end{smallmatrix}$

Table 1.

confinement volume in the solar vicinity (Box 1), and hence have a spectral index near to 3 (see Fig. 1). Our prediction is not in contradiction with the existing data(5). However, it is suggested to make improved measurements to examine the prediction presented above.

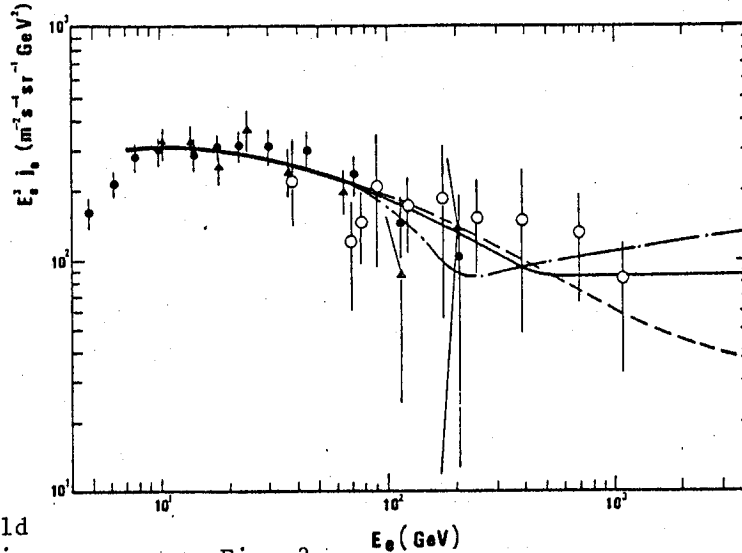


Fig. 3

only originate from their confinement volume in the solar vicinity (Box 1), and hence have a spectral index near to 3 (see Fig. 1). Our prediction is not in contradiction with the existing data(5). However, it is suggested to make improved measurements to examine the prediction presented above.

## References:

- Ormes, J. and Protheroe, R.J. 1983, Ap. J., 272, 756.
- Tan, L.C. and Ng, L.K. 1983, Ap. J., 269, 751.
- Strong, A.W. et al., 1978, M.N.R.A.S., 182, 751.
- Tan, L.C. 1985, Ap.J., 1985, in press.
- Nishimura, J. et al., 1980, Ap. J., 238, 394.
- Prince, T.A. 1979, Ap. J., 227, 676.
- Muller, D. and Tang, J. 1983, Proc. 18th Internat. Cosmic Ray Conf. (Bangalore), 2, 60.
- Holmes, J.A. 1974, M.N.R.A.S., 166, 155.